UDC 621.391:681.32

TIME–FREQUENCY DECOMPOSITION OF SEISMIC SIGNALS BASED ON SHORT TIME FOURIER TRANSFORM

This paper is dedicated to Prof. Ilija Stojanović on the occasion of his the 75th birthday and the 50th anniversary of his scientific work

Vidosav Stojanović, Miomir Stanković and Igor Radovanović

Abstract. The squared module of short–time Fourier transform (STFT) called spectrogram (SPEC) is used for decomposing the seismic signal energy into the time–frequency (TF) plane. The SPEC is calculated by using a window function which width is determined by duration of the excitation signal. The seismic signal energy distribution is observed and the definition of the energy center frequency is given. After making a number of experiments with the seismic signals obtained from the hit of the metal sphere against the lawn, both the mean value of the energy center frequency and the standard deviation are found and given in terms of the distance between the detector and the place of excitation. Both functions decrease as distance increases, so it is possible to estimate the distance using only one detector. These results are useful for seismic signal analysis when several excitations occur. This is demonstrated in the analysis of seismic signals obtained from two sphere excitations. A signal obtained from a car is also analyzed. It is presented that the seismic signal energy center frequency obtained from the car excitation occurs at frequencies higher than those obtained from the sphere. Accordingly, the car and the metal sphere identification, when both excitations occur at the same time, is made.

1. Introduction

Time-frequency representations are widely used for the nonstationary signal analysis. They perform a mapping of an one-dimensional signal of time into a two-dimensional function of time and frequency, in order to extract

relevant information. The standard Fourier analysis allows the decomposition of the signal into individual frequency components and establishes the relative intensity of each component. However, it is not possible to extract the information when a particular spectral component occurred. If we break up a signal into short time intervals using window function, Fourier analyze each interval and slide the window along the time axis, energy distribution can be calculated. This transformation is called short–time Fourier transform (STFT) [1]–[3]. The energetic version of this transform obtained as squared module of the STFT is referred to as spectrogram (SPEC). This transform has well known properties inherited from the Fourier transform [4], but has not simultaneously good time and frequency resolutions. Better TF resolution can be achieved using bilinear TF distributions [5]–[9], but their main drawback is that cross terms might occur at the position of auto-terms involving ambiguity in the TF plane. Because of simplicity of implementation the SPEC is more widely used for the nonstationary signal analysis.

The aim of this paper is to identify different types of excitations using TF analysis of seismic signals obtained from these excitations. The signals of car and sphere are analyzed using STFT. The sphere is used instead of pedestrian because the sphere signal shape in time domain resembles the pedestrian signal and is easier to manage with.

The influence of the window width on SPEC resolution is shown. A good time resolution is achieved by an appropriate selecting of the window width while frequency resolution, defined as the frequency axis number of samples, is enhanced by zero padding the product of seismic signal and a window function.

The energy of seismic signals is centered around the maximum point in the TF plane which represents the energy center. Varying the distance between the detector and the place of excitation the energy center frequency deviates. For the number of seismic signals obtained on the flat soil covered with grass, the energy center frequency in terms of the distance, is found. As distance increases, so does the energy center frequency decrease for both types of excitations. This especially stands for sphere signal for which it is possible to estimate the distance from the detector. It is shown that the car seismic signal energy exists at lower frequencies than one obtained from the sphere signal. Accordingly, a car and sphere identification, when both excitations occur at the same time, is made.

The organization of this paper is as follows: Section 2. briefly presents definition of STFT, and its square module, SPEC. The influence of the window function width on time and frequency resolution is also presented.

Section 3. consists of four subsections: Subsection 3.1. describes the system for the acquisition and seismic signal processing. The width selection of the window function depending on an excitation signal duration is presented in Subsection 3.2. In Subsection 3.3. the energy center frequency of a sphere is given in terms of the distance from the detector. Subsection 3.4. provides moving car and metal sphere identification when these excitations occur at the same time.

2. Background of Time-frequency Analysis

The short-time Fourier analysis has been the most widely used for the time-frequency analysis [10], [11]. If $s(t)$ is a real signal, in our case it is a seismic signal, then spectrogram or the squared module of the STFT is defined by

$$SPEC_s(t,\omega) = \left| \int_{-\infty}^{+\infty} s(\tau)w(\tau - t)e^{-j\omega\tau}\ d\tau \right|^2 , \qquad (1)$$

where $w(t)$ is a window function. The spectrogram maps the signal $s(t)$ from the time domain to the time–frequency domain and presents its energetic distribution function. It can be considered as the convolution of the input signal $s(t)$ and the impulse response of a bandpass filter $w(t)e^{-j\omega t}$, with its center frequency ω. This transform is bilinear, positive and a member of the Cohen class of distributions [8].

In the frequency domain, the corresponding definition of the spectrogram is

$$SPEC_s(t,\omega) = \frac{1}{2\pi} \left| \int_{-\infty}^{+\infty} S(\theta)W(\theta - \omega)e^{j(\theta-\omega)}d\theta \right|^2 , \qquad (2)$$

where $S(\omega)$ and $W(\omega)$ are the Fourier transforms of $s(t)$ and $w(t)$, respectively. Thus, the spectrogram can be considered as a result of passing the signal $s(t)$ through a bank of band-pass filters $W(\theta - \omega)$ with constant bandwidth and mother filter $W(\omega)$. This shape of the spectrogram can be used to study the behavior of the signal properties around the frequency point ω.

Both definitions of spectrogram can be used equally, but the definition in frequency domain requires window function representation in Fourier domain and so is harder to implement.

The ability to resolve two signals with the same frequency appearing at different instances of time i.e. the ability to resolve two signals with different frequencies appearing at the same time represents time and frequency resolution, respectively. The time and frequency resolutions of SPEC depend on the width of the window $w(t)$. Therefore, SPEC suffers from the well-known tradeoff between time and frequency resolutions. On one hand, a good time resolution requires a short window $w(t)$, on the other hand, a good frequency resolution requires a narrow–band filter $W(\omega)$ i.e. a long window $w(t)$. The product of time and frequency deviations of the window function and its Fourier transform which defines join time–frequency resolution [12], must satisfy Heisenberg's Uncertainty Principle [7]

$$\sigma_t \sigma_\omega \geq \frac{1}{2}. \tag{3}$$

In common usage σ_t and σ_ω are called the duration and the bandwidth of a signal.

The joint time-frequency resolution does not depend on the width of the window $w(t)$ but depends on the window's shape. The best choice of window is the Gaussian window because it reaches the boundary of equation (3), [13], [14]. The Gaussian window is

$$w(t) = \begin{cases} \exp\left(-\frac{t^2}{\beta}\right) & -T_o/2 \leq t \leq T_o/2 \\ 0, & \mid t \mid > T_o/2 \end{cases} \tag{4}$$

where β is a positive real number, called scaling factor and T_o is the width of the window. The scaling factor affects on the window shape i.e. on the passband of NF filter.

The definitions of the SPEC and the Gaussian window in discrete domain are

$$SPEC_s(n, k) = \left| \sum_{l=0}^{N-1} s(n+l)w(l)e^{-j\frac{2\pi}{N}kl} \right|^2, \quad k = 0, 1, 2, \ldots, N-1, \tag{5}$$

and

$$w(n) = \exp\left(\frac{-\left(n - \frac{N-1}{2}\right)^2}{\beta}\right) \qquad n = 0, 1, 2, \ldots, N-1. \tag{6}$$

where n and k represent the indexes associated with time and frequency, respectively.

The SPEC is obtained by truncating the analyzed signal $s(n)$ with the window function $w(n)$ centered at any particular time of interest, calculating its Fourier transform, and sliding the window along the time axis [15]. In discrete domain the SPEC is even, positive and periodic function in frequency with a period of 2π. The radix–2 fast Fourier transform algorithms, described by Burrus and Sorensen [16], [17], were used for SPEC calculation.

3. Acquisition and Analysis of Seismic Signals

A body that possesses kinetic energy in the moment of hitting the ground and generates seismic waves propagating through the ground in all directions is referred to as an excitation. The excitations analyzed in this paper are metal spheres 8 kg in weight, which fall free, and a car that moves on the flat soil covered by grass. The surface waves which radially propagate from the place of excitation are of the main importance since their magnitudes are much higher than one obtained from body waves [18]-[20]. The shape, magnitude and velocity of seismic signals depend on the type of the excitation, soil structure and the distance between excitation and a place where waves are detected.

3.1. System Description

The system for acquisition and analysis of seismic signals is displayed in Fig. 1. It consists of a vibration detector, filters, amplifiers and DSP card mounted on a PC which monitors results.

The seismic waves are detected by a passive vibration detector which produce voltage waveforms, referred to as seismic signals. These signals correspond to the vertical velocity of motion of the earth's surface in response to seismic waves [13]. The resonant frequency of the detector is low and the bandwidth is $10 - 200$ Hz. The detected signal is going to an instrumental amplifier with a gain of about 10 dB. The filter is an active bandpass sixth order Chebyshev filter with the following parameters: the cut–off frequencies are 10 and 200 Hz, gain 18 dB and minimal passband attenuation 1 dB. After filtering, the signal is amplified again by a two section amplifier with the total gain of 60 dB.

The analog signal with the magnitude range from $-5V$ to $+5V$ is going to the DSP card from the output of the amplifier. This card includes a 14-bit programmable A/D converter, RAM, and a DSP signal processor with its interfaces. The DSP processor used is the TMS320C30 of Texas Instruments.

The seismic signals are sampled with the frequency of $f_s = 1$ KHz and the samples are stored in data block with the length of N. The SPEC of
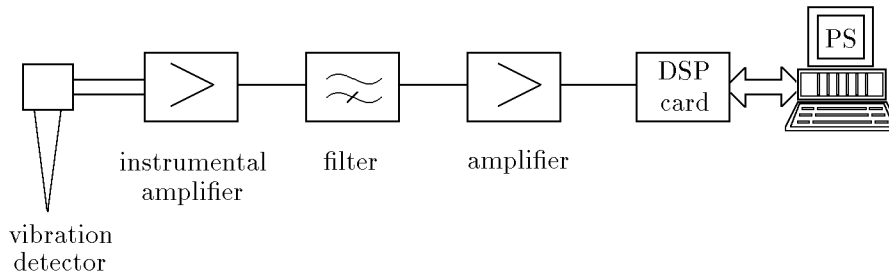
Fig. 1. Block diagram of the system for aquisition
and analysis of seismic signals.

seismic signal is calculated at any instant of time by Fourier transform of the product of this data block and the window function. All these operations are performed on the DSP card. The data vector of SPEC is stored in PC memory through the bus and displayed on monitor.

3.2. Selection of the Window Function

The proper selection of Gaussian window width N is needed when seismic signal analysis is performed using SPEC. The scaling factor β in (6) depends on N and is given as $\beta = 0.1N^2$. The maximal attenuation of the first side lobe, for this value of β is 35.5 dB. Assume that two same excitations occur one by another with the delay equal to duration of each of them. The demand which needs to be satisfied in the window width selection is to identify these excitations using contour plot of SPEC of such signal.

In order to determine excitation signal duration let us observe a seismic signal obtained from the metal sphere which fall free from the height of 1 m. The distance between the place of excitation and the detector is 15 m. The normalized signal within the interval of 1 s is shown in Fig. 2. The excitation signal occurs at the beginning of this interval in the form of decaying sine wave. The rest of the interval is fulfilled with the terrain noise. The noise level depends on the terrain configuration, distance from the urban areas, roads, rivers etc. The frequency of this noise is equal to or greater than 50 Hz.

In order to select the width of the window $w(n)$, excitation signal duration is needed to be determined. In time interval, much longer than 1 s the noise magnitude is rather constant while signal magnitude depends on the type of the excitation and its distance from the detector. As distance
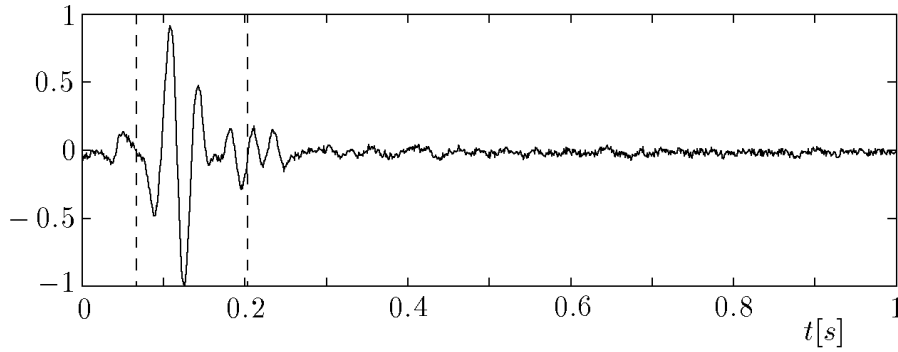
Fig. 2. The excitation signal selection.

increases, so does the magnitude decrease as well as the signal to noise ratio. This means: the higher amplification, the higher noise level. The absolute value of normalized noise, presented in Fig. 2 is $V_n = 0.1$. The excitation signal is a part of seismic signal satisfying $|s(n)| > V_n$. Using this fact we can find the excitation signal duration. The threshold level V_n is higher for long distances from the detector which affects the excitation signal duration to be shorter. That is the reason we have to find the maximum noise level. If the longest distance from the detector is 30 m the threshold level V_n is $V_n = 0.2$. This threshold level determines excitation signal duration.

The beginning of the excitation signal is the first zero–crossing moving backwards from the moment when signal exceeds threshold level V_n and the end is the first zero–crossing moving upwards from the moment when signal magnitude falls below the same threshold level. In the successive time interval of $T_{max}/2$ must stand that $|s(n)| \leq V_n$, where $1/T_{max}$ is the minimal signal frequency. This frequency equals lower bandpass cutoff frequency $1/T_{max} = 10\ Hz$. The excitation signal duration interval obtained by proposed procedure is shown in Fig. 2, where the beginning and the end of the interval are presented with dash lines. This interval is $T_e = 136\ ms$ long.

In order to make a proper window width selection assume that the excitation signal, shown in Fig. 2, occur twice. The delay of the second occurance is equal to the duration of the excitation signal. With this signal we are approximating two different excitation signals occuring one by another.. A time shape of such signal is shown in Fig. 3.

Assume that the width of the Gaussian window is $N = 128$. The mesh and contour plots of SPEC obtained using (5) and (6), are presented in Figs. 3(b) and 3(c), respectively.
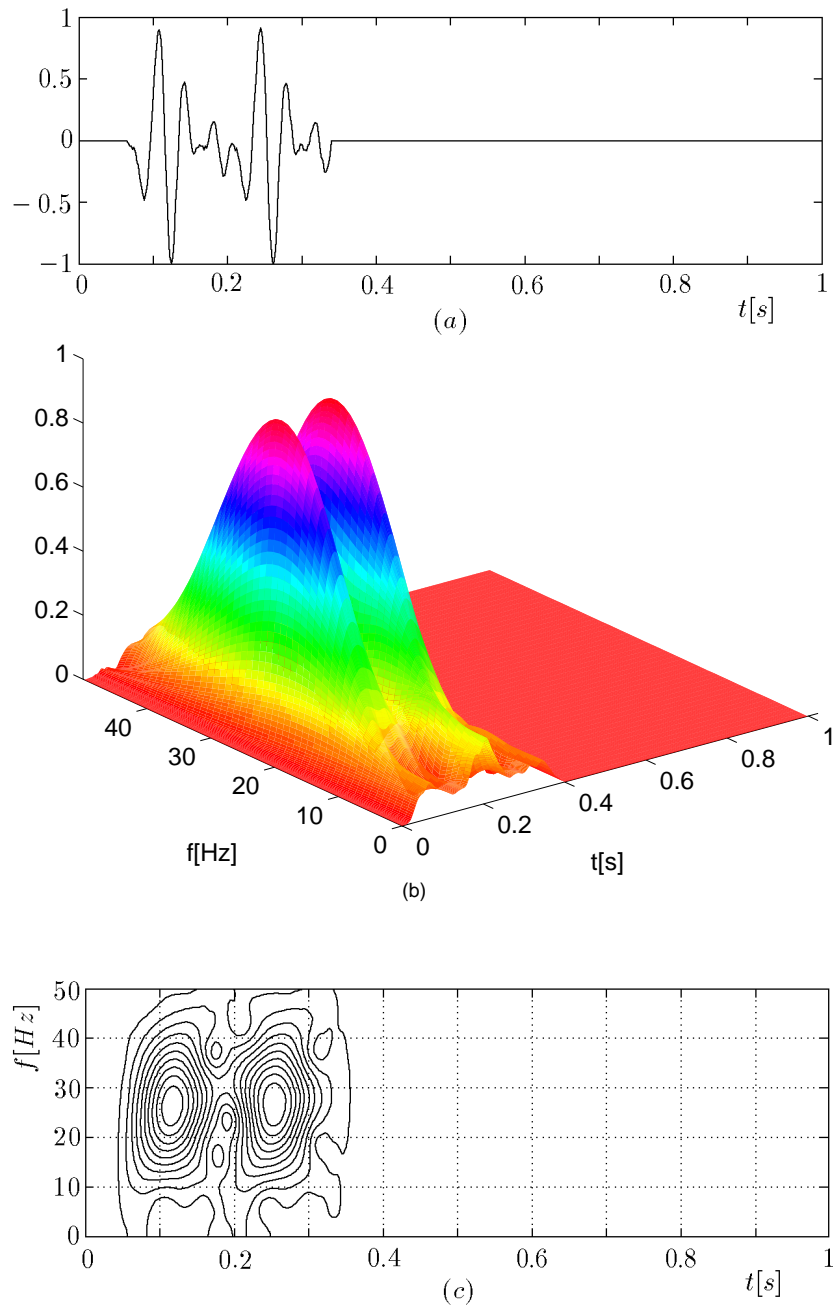
Fig. 3. The seismic signal made of two excitation signals is shown in a), the spectrogram is shown in b) as a mesh plot and in c) as a contour plot.

The maximal frequency coordinate of SPEC presented in this and further examples is 50 Hz, because no signal component occurs at frequencies above this one. It can be seen from the picture that there exist two hills with the picks around $(t_1, f_1) = (0.116 \ s, 26.37 \ Hz)$ and $(t_2, f_2) = (0.254 \ s, 26.37 \ Hz)$. The second hill is higher than the first one because most of the excitation signal energy is concentrated in the second half of the interval T_e. If the excitation signal energy concentration is symmetrical in the interval T_e the height of both hills would be equal and difference $t_2 - t_1$ would be equal to excitation signal duration T_e i.e. to delay between these two excitation signals. There is a valley between two hills occurring at the time $(t_3 = 0.187 \ s$. The coordinate and the height of this valley depend on the signal shape and the window function width. The affection of the window function width on SPEC resolution can be expressed as follows

$$\xi(N) = \frac{SPEC_s(t_3, \omega_3)}{SPEC_s(t_2, \omega_2)}, \tag{7}$$

where $SPEC_s(t_3, \omega_3$ is a maximal value of SPEC at the instant of time when valley occur and $SPEC_s(t_2, \omega_2$ is the SPEC value at the top of the higher hill.

Expression (7) stands only if two hills occur in SPEC. Parameter ξ in terms of the window function width, for the signal presented in Fig. 3(a), is shown in Fig. 4. This curve has wave form. A maximal window width is obtained when both heights of the valley and the hill are equal. Further increasing of the window width will produce merging of two hills into one. The value of the ξ parameter is equal to 1 if the width of the window is maximal $N_{max} = 252$. The frequency of minimum occurring is equal to reciprocal value of the excitation signal dominant frequency $2\pi/\omega_1$. It can be seen from the picture that waveform envelope decreases as the time resolution increases i.e. as the window width decreases. A minimal window width is determined with the excitation signal dominant frequency. This means that SPEC of the seismic signal is almost equal to instant signal energy shape for the window width that is less or equal to T_{max}. In this case several hills occur in SPEC so expression (7) can not be used for parameter ξ calculation.

The window width can be determined analyzing the Fig. 4. For excitation signal identification the clipping level of SPEC should exceed the maximal valley height in order to have two island in the contour plot. This clipping level should also be higher than noise energy level $V_n^2 = 0.01$. Assume that clipping level is 0.2. According to Fig. 4 the minimal window width is $N = 159$.

Changing the distance from the detector the excitation signal duration varies a little. The proposed procedure for the window width determination, for the signals obtained at different distances from the detector is repeated a number of times. The distance from the detector varied from 5 m to 30 m with the 1 m step. The hitting place was equidistantly moved along the line. For each distance, fifty acquisitions were performed and both, mean value of the excitation signal duration and the window width were calculated. The obtained results are $\overline{T}_e = 155$ s and $\overline{N} = 133$. Since radix-2 algorithms [10], [11] are used in Fourier transform calculation, in further analysis we use window width $N = 2^7$.

The proposed procedure for window width selection provides a good time resolution. The set of frequencies for which SPEC is evaluated is $\omega_i = (2\pi\Delta f/f_s)i$, where $i = 0, 1, \ldots$ and $\Delta f = f_s/N = 7.8125$ Hz. As Δf decreases, the window width increases enhancing the frequency resolution. However, zero-padding the product of a window and the signal with $Z-$points, and taking an FFT of a higher order than window length will increase the number of samples in the SPEC in the frequency domain.
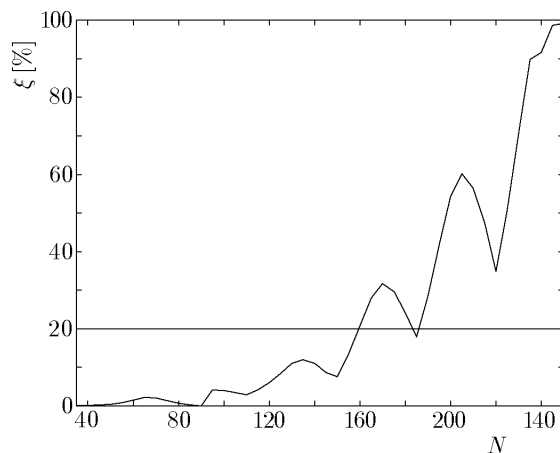
Fig. 4. Parameter ξ in terms of the window width.

We obtained a better visual picture, because the Fourier transform has smoother continuous transitions in the frequency domain. Assume that $\Delta f \leq 1$ Hz. The Fourier transform of the data block is $P = N + Z \geq 1000$ samples long. In further analysis we assume that $P = 1024$ and $\Delta f = 0.9765$ Hz.

3.3. The Energy Center Frequency

We have already seen in subsection 3.2 that in 3–D representation of SPEC the hills occur. These hills represent the energy located in domain centered on point (t, f), which is in fact the top of the hill, and referred to as energy center of seismic signal. The time and frequency coordinates correspond to the instant of time when excitation is acting and dominant spectral component of the signal in that instant of time, respectively. After making a number of experiments it is shown that the energy center frequency coordinate depends on the distance from the detector. According to experiments described in previous section, in which the window function width is selected, a main energy center frequency is calculated in terms of the distance from the detector. The main value is displayed as a solid line in the shaded areas of Fig. 5. The spread about the mean value known as the standard deviation describes how far the measured values of energy center frequencies are from the mean value. The distribution of these values is Gaussian. The shaded areas presented in figures 5 lie between $\pm 3\sigma$ boundaries, where σ presents the standard deviation of measured values.
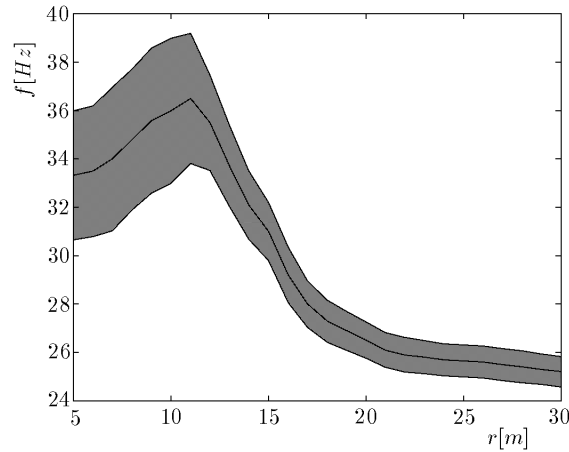
Fig. 5. The mean and the standard deviation of the energy center frequency.

At short distances, up to 13 m, both the mean value and the frequency deviation increase. In the rest of the interval they both decrease. The energy center frequency is in the range from 31 Hz to 39 Hz, at the short distances. For distances longer than 17 m this frequency is in the range from 25 Hz to 30 Hz. It can be noticed from the figure that for the long distances, both the energy center frequency and the deviation are low.

The metal sphere energy in the moment of hitting is proportional to the height from which the metal sphere falls free. This height has not been changed in any of previous experiments so it was not possible to consider its influence on the energy center frequency coordinate. Changing the distance between the sphere and the detector and height of the sphere i.e. its potential energy, it was inferred that energy center frequency does not depend on energy. The only parameter that varies is the magnitude of the seismic signal.

According to results shown in Fig. 6 the distance between detector and the place of excitation can be estimated along the line where excitation occurs. With no doubt we can only estimate whether excitation occurs at the short or long distance.

Changing the direction along which excitation occur the energy center frequency changes a little, because of the different structures of soil around the detector. If acquisition is performed in only one direction, the deviation of energy center frequencies from the main value is minimal.

Look at the following examples. The seismic signals are obtained from the hits of two metal spheres that fall free, against the lawn. In the first example, distances between hitting places of both spheres and the detector were the same (10 m). The second sphere hits the ground about 150 ms later than the first one. In the second example, both spheres touched the ground at the same time but they were at different distances. The distances of the first and second sphere were 7 m and 30 m, respectively. In order to achieve the same magnitude of signals, the first sphere fell from the height of 0.2 m and the second one from the height of 2 m. The time shape of the seismic signal, a mesh plot and a contour plot of the SPEC, for both examples, are shown in figures 7 and 8 under (a), (b) and (c), respectively.

In the second example, the seismic wave obtained from the second sphere was detected about 150 ms later than one obtained from the first sphere as can be viewed in Fig. 8(a). The arrival times of signals differ because of the finite rate of propagation of the seismic waves through the ground.

It can be noticed that the shapes of seismic signals in time domain in both examples are very similar. However, after TF analysis of both signals it is obvious that energy center frequencies differ. From the figures 7(b) and 7(c), it can be noticed that the coordinates of centers for the first signal are (0.148 s, 36.13 Hz) and (0.301 s, 37.11 Hz). The coordinates for the second signal are (0.121 s, 34.18 Hz) and (0.298 s, 23.44 Hz), and are shown in figures 8(b) and 8(c). It can be noticed from the Fig. 6 that the distances for both spheres in the first example were at the short distance, while for

the second example, the first sphere was at short and second one at long distance.

3.4. The Excitation Signal Obtained from a Car

Let's have a look at the seismic signal obtained by a vehicle moving along the flat soil covered with grass. The energy of tires acting on the soil surface depends on the weight and velocity of the vehicle, as well as flatness of the soil on which vehicle is moving. If terrain is perfectly flat the energy is transmitted to the ground in the moments of starting and stoping of the car. The engine also generates acoustic waves and vibrations that propagates through the soil in the form of seismic waves. There are bumps and recesses existing on the soil in real cases. The seismic signals are generated when a vehicle is passing over these prominences. The number of bumps and recesses is often high so the detector is constantly activated making the seismic signal envelope rather constant. Since energy center frequency does not depend on excitation energy we can use any kind of vehicle. In the following experiments we used a car.

A seismic signal obtained by the car is shown in Fig. $8(a)$. This signal is recorded during the car movement along the line normally located 10 m away from the detector. The signal magnitude increases and decreases when the car is moving toward and from the detector, respectively. Fig. $8(a)$ represents part of the signal when the car was nearly to the detector. A SPEC of the car seismic signal is calculated using (5) and (6) and its mesh and contour plots are shown in Figs. $8(b)$ and $8(c)$, respectively. It can be noticed that the signal envelope is rather constant.

There are three energy centers with the equal frequency coordinates located around 19 Hz. The energy center frequencies of the seismic signals obtained at longer distances from the detector are very similar to this. After making a number of experiments, described in Subsection 3.1. we inferred that the energy center frequency varies a little with the distance. Changing the distance between the car and the detector from 5 m to 30 m we inferred that energy center frequencies are in the range from 20 Hz to 17 Hz. This means that the car and sphere energy center frequencies do not overlap in TF plane. Using this fact it is possible to identify the car and the sphere if both excitations occur at the same time.

The excitation identification is hard to make in two cases: First, when the sphere seismic signal magnitude is less than or equal to the car seismic signal magnitude and second, when the sphere magnitude is much greater than car magnitude. In other cases the identification is simple due to confirmation of sphere and car presence in both time domain and TF plain.
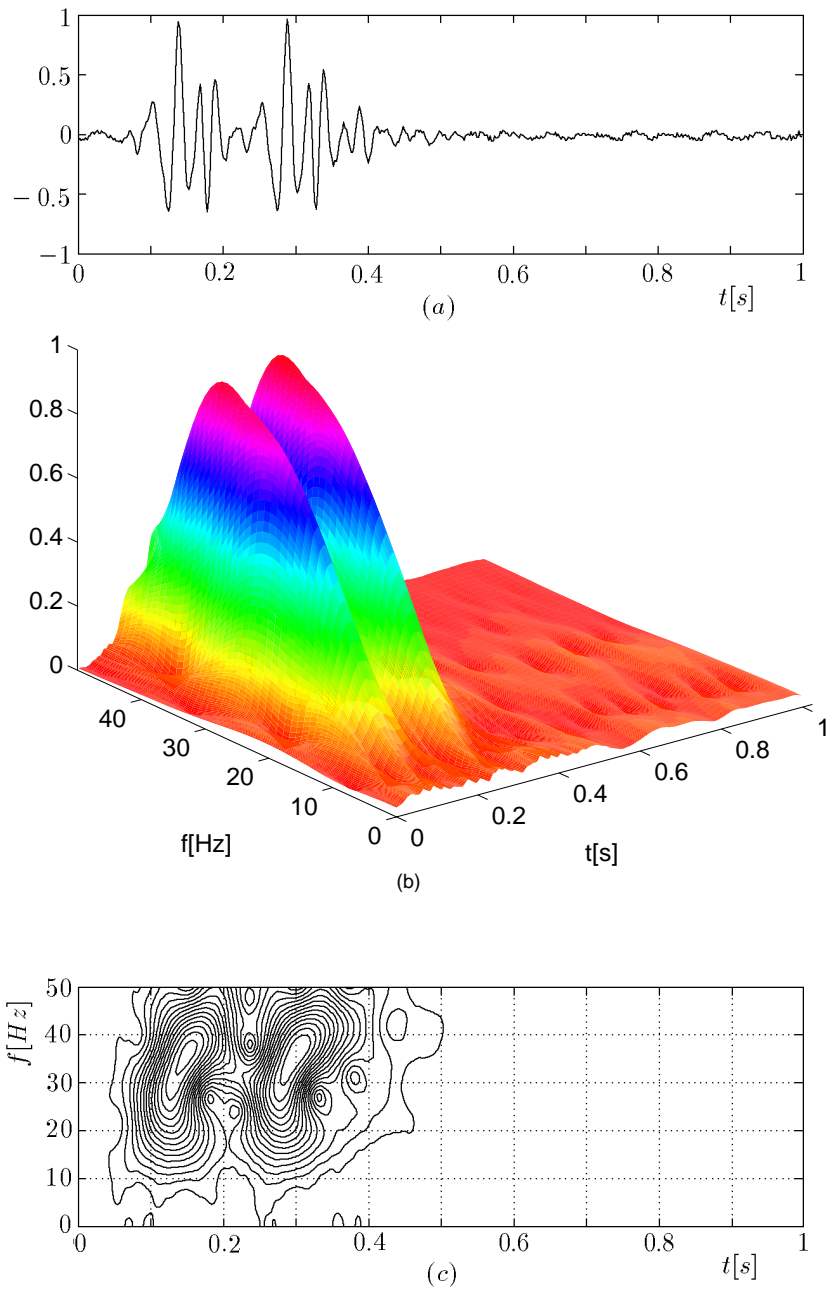
Fig. 6. *The seismic signal with two excitations occurring at the different time, is shown in (a), the SPEC is shown in (b) as a mesh plot and in (c) as a contour plot.*

(a)

(b)

(c)
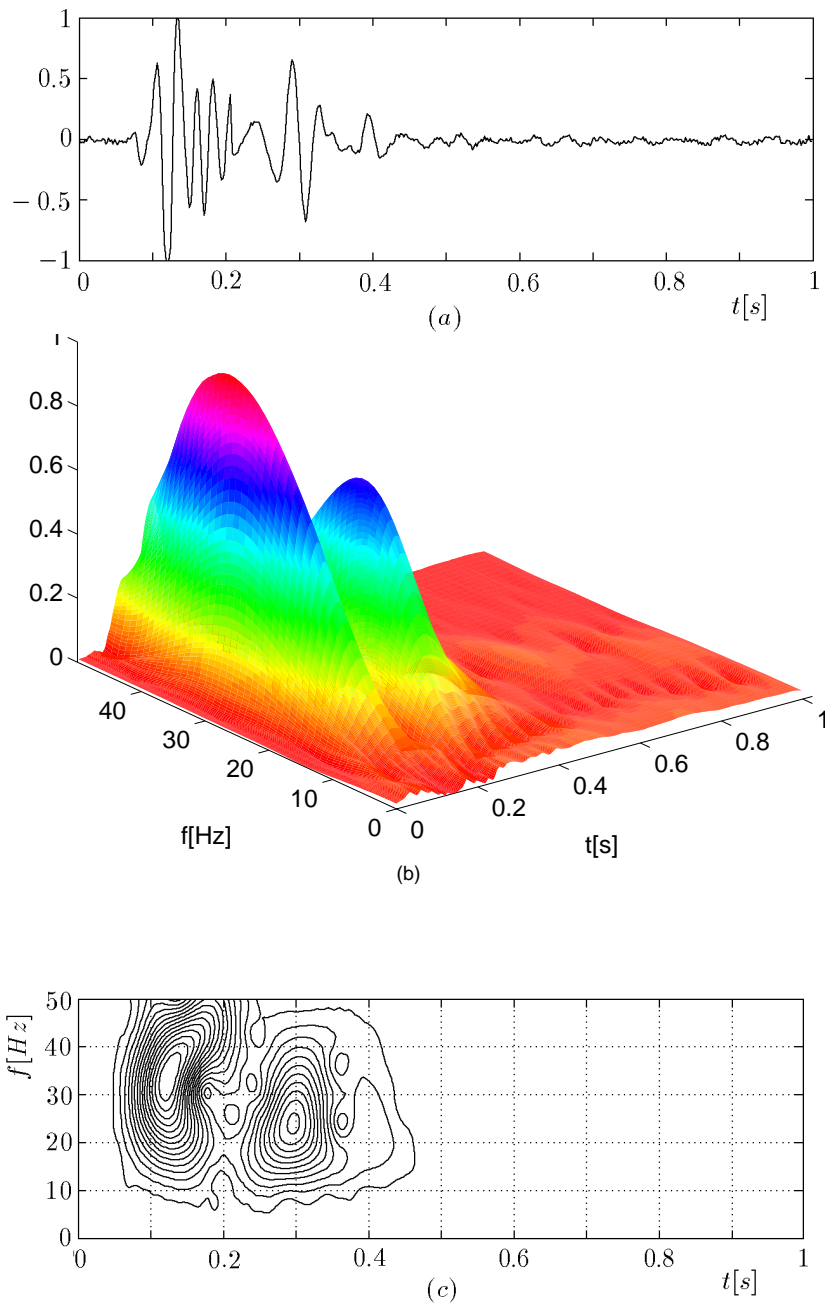
Fig. 7. *The seismic signal with two excitations occurring at the same time, is shown in (a), the SPEC is shown in (b) as a mesh plot and in (c) as a contour plot.*

A seismic signal representing this case is shown in Fig. 9(a). Observing the shape of this seismic signal in the time domain the presence of the car and sphere is obvious. The magnitude of car signal is rather constant during the whole interval while sphere presence is followed with increasing the signal magnitude in particular instances of time. As seen in Figs. 9(b) and 9(c) the frequency coordinates of energy centers for the sphere and the car are 24 Hz and 17 Hz, respectively.

The seismic signal, representing the first case for which the identification is hardest, is shown in Fig. 10(a).

In this experiment, the sphere was falling from 2 m. The distances were 30 m for the car, and 20 m for the sphere. It is very difficult to remark the affection of the sphere in Fig. 10(a). The shape of the signal, presented in this figure is quite similar to the one obtained by the car because the signal envelope is almost constant along the proposed period. However, calculating the SPEC and using its mesh and contour plots the two excitations are easy to remark. The mesh and contour plots are shown in Figs. 10(b) and 10(c), respectively. The energy centers occurring at 20 Hz are the result of the car excitation while the one at $(t, f) = (0.43\ s, 25.39\ Hz)$ is the result of sphere excitation. The deference between the car and sphere signal energy centers are much greater at shorter distances making the identification much easier.

Fig. 11(a) presents a car seismic signal for the second case. The presence of the sphere excitation is obvious since there exist intervals with the high seismic signal magnitude value. The presence of the car seismic signal is very difficult to remark since its shape strongly resembles the noise. However, mesh and contour plots of SPEC of this signal, presented in Figs. 11(b) and 11(c), respectively, show that energy center frequencies occur in the range from 17 Hz to 20 Hz. In the case of terrain noise the energy center frequencies are around 50 Hz.

4. Conclusions

The choice of the window function width is very important in SPEC seismic signal analysis. This width is determined by the time resolution of SPEC of the seismic signal obtained from the free fall of two metal spheres. The condition that has to be fulfilled is to identify the excitations by the contour plot analysis of SPEC of such signal in TF plane. Since the frequency resolution is not of prime importance, a good localization of energy center frequency is achieved by zero–padding the product of a seismic signal and a window function. In this paper, the seismic signals of car and spheres were analyzed.
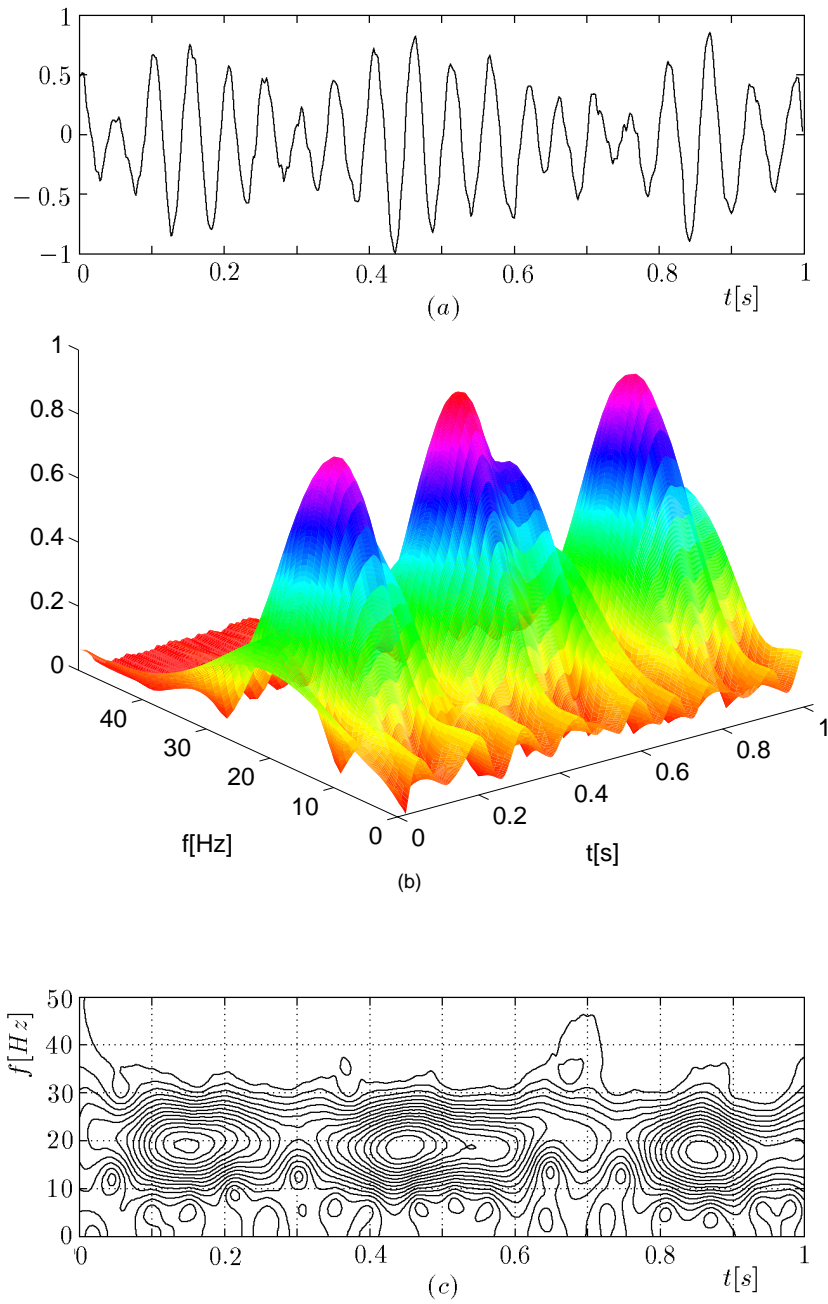
Fig. 8. The seismic signal of moving car is shown in (a),
the SPEC is shown in (b) as a mesh plot and in (c)
as a contour plot.
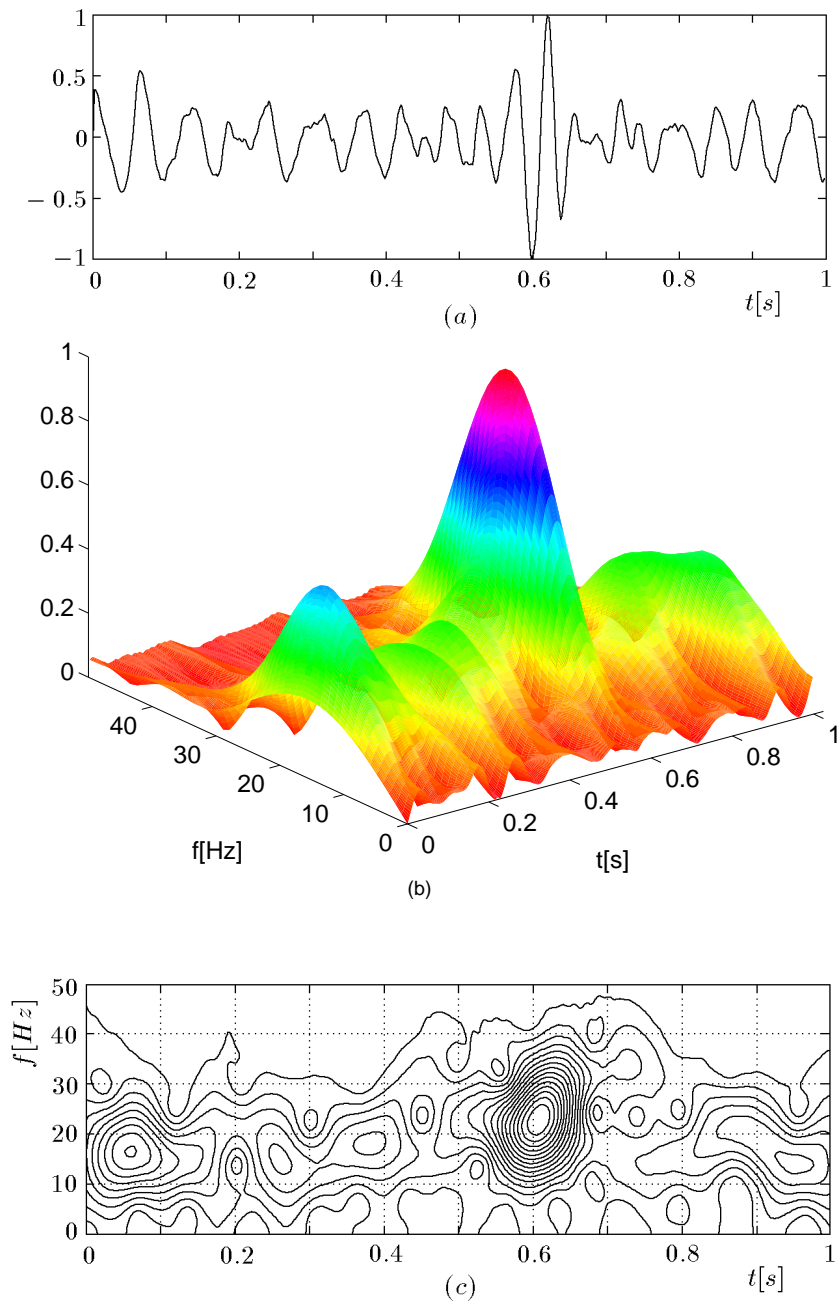
Fig. 9. *The seismic signal obtained from the moving car and metal sphere*
       is shown in (a), the SPEC is shown in (b) as a mesh
       plot and in (c) as a contour plot.
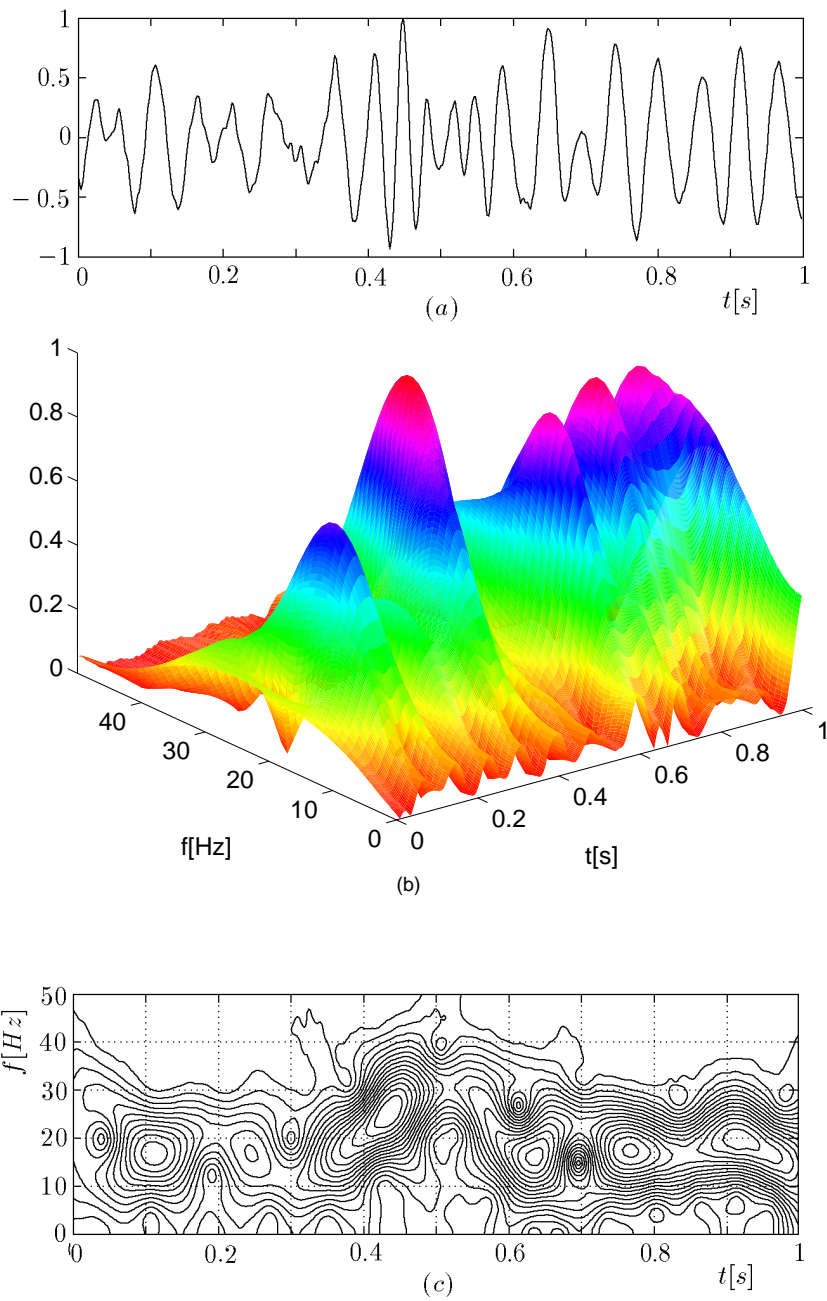
Fig. 10. The seismic signal obtained from the moving car and metal sphere
for the case 1, is shown in (a), the SPEC is shown in (b) a mesh
plot and in (c) as a contour plot.
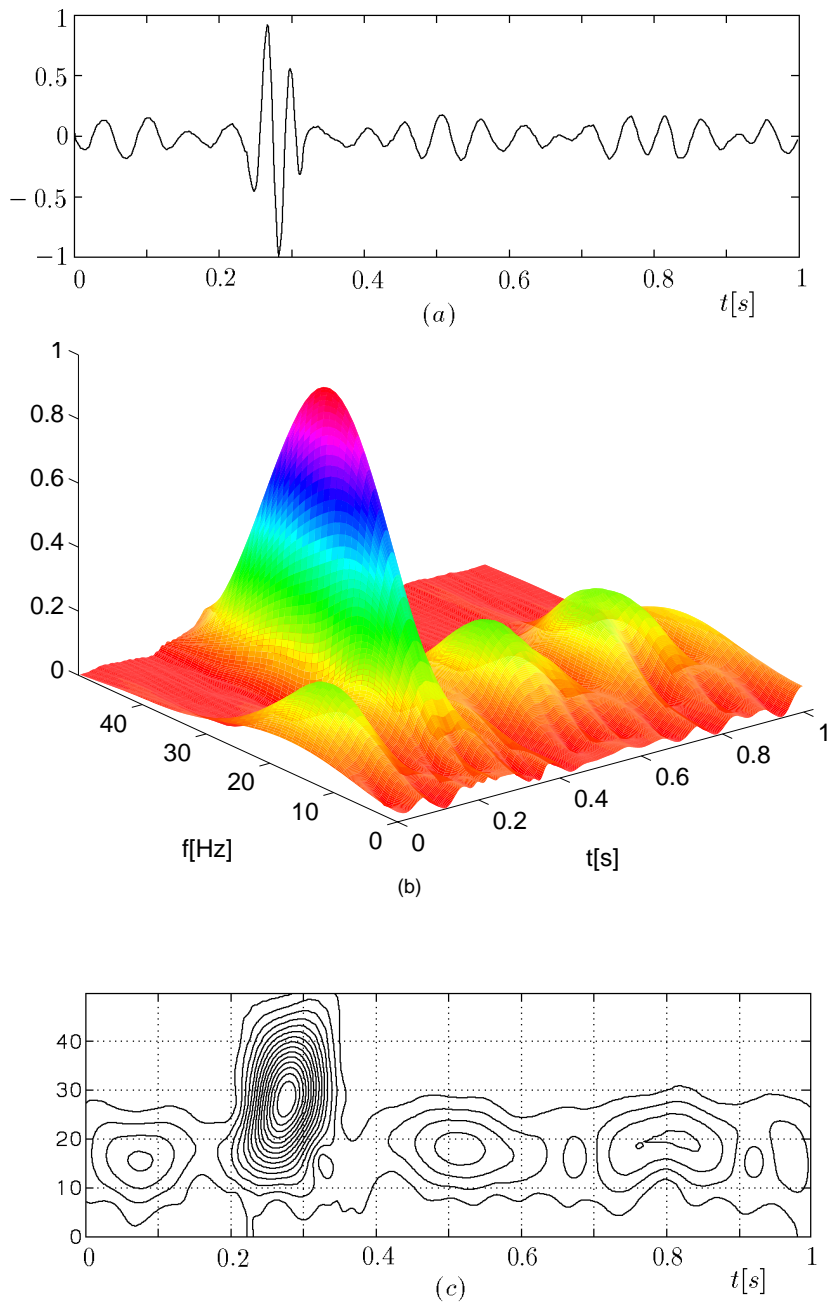
Fig. 11. *The seismic signal obtained from the moving car and metal sphere*
for the case 2, is shown in (a), the SPEC is shown in (b) as a mesh
plot and in (c) as a contour plot.

After making a number of experiments it is shown that the seismic signal energy center frequency depends on the distance from the detector and decreases as distance increases. This especially stands for the sphere seismic signals for which energy center frequency is given in terms of the distance. Accordingly, the distance from the detector can be estimated using only one detector. The location of a car and a sphere seismic signal energy differ in TF plane because the car seismic signal energy is located at lower frequencies. This is used in the car and sphere identification when both excitations occur at the same time.

The results given in this paper stand for flat soils covered with grass like parks, meadows, glades etc. Determinating of the energy center frequencies in terms of the distance for other types of soil needs further analysis.

R E F E R E N C E S

1. J. B. ALLEN: *Short term spectral analysis, synthesis, and modification by discrete Fourier transform.* IEEE Trans. Acoust., Speech, Signal Processing, vol ASSP-25, pp. 235-238, June 1977.

2. J. B. ALLEN AND L.R. RABINER: *A unified approach to short-time Fourier analysis and synthesis.* Proc. IEEE, vol. 65. 1977. pp 1558-1566, Nov. 1977.

3. M. R. PORTNOFF: *Time-frequency representation of digital signals and systems based on short-time Fourier analysis.* IEEE Trans. Acoust., Speech, Signal Processing, vol. ASSP-28, pp. 55-69, Feb. 1980.

4. M. J. BASTIAANS: *A sempling theorem for the complex spectogrm, and Gabor's expansion of a signal in Gaussian elementary signals.* Optical Engineering, vol. 20, no. 4, pp. 594-598, July,August 1981.

5. T.A.C.M. CLAASEN AND W.F.G. MECKLENDBRAUKER: *The Wigner distribution, a tool for time-frequency analysis, Part I: Continuous-time signal.* vol. 35 no. 3 pp. 217-250; *Part II: Discrete-time signals*, vol. 35 no. 4/5, pp. 276–300; *Part III: Relations with other time-frequency signal transformations*, Philips J. Res., vol. 35, no. 6, pp. 372–389, 1980.

6. H. CHOI AND W. J. WILLIAMS: *Improved Time-Frequency Representation of Multicomponent Signals Using Exponential Kernels.* IEEE Trans. Acoust., Speech, Signal Processing, vol. 37, no. 6, pp. 862-871, June 1989.

7. L. COHEN: *Time-Frequency Distributions - A Rewiev.* Proc IEEE, vol. 77, no. 7, pp. 941-981 July 1989.

8. I. DAUBECHIES: *The wavelet transform, time-frequency localization, and signal analysis.* IEEE Trans. Inform. Theory, pp. 961-1005, September 1990.

9. W. RIHACZEK: *Signal energy distribution in time and frequency.* IEEE Trans. Inst. Radio Engineers, vol. IT-14, pp. 369-374, 1968.

10. M. R. PORTNOFF: *Implementation of the Digital Phase Vocoder Using the Fast Fourier Transform.* IEEE Trans. Acoust., Speech, Signal Processing, vol. ASSP-24, no. 3, pp 243-248, June 1976.

11. L. R. RABINER AND J. B. ALLEN: *On the Implementation of a Short-Time Spectral Analysis Method for System Identification.* IEEE Trans. Acoust., Speech, Signal Processing, vol. ASSP-28, no. 1, pp. 69-78, Feb. 1980.

12. S. QIAN AND D. CHEN: *Joint Time-Frequency analysis.* Englewood Cliffs, NJ: Prentice-Hall, 1996.

13. A. J. E. M. JANSSEN: *Optimality property of the Gaussian window spectogram.* IEEE Trans. Signal Processing, vol. 39, no. 1, pp. 202-204, January 1991.

14. H. R. ANDERSON, R. CAMATTA, C. DUPONT, E. RINGÖEN AND J. ÖSTERGAARD: *The Gabor Spectogram and its Application in Time–Frequency Analysis of Bat Sonar.* AAlborg University, Institute of Electronic Systems, January 1997.

15. M. J. BASTIAANS: *On the sliding-window representation in digital signal processing.* IEEE Trans. Acoust., Speech, Signal Processing vol. ASSP-33, no. 4, pp. 868-873, August 1985.

16. C. S. BURRUS AND T. W. PARKS: *DFT/FFT and convolution algorithms.* New York, Wiley, 1985.

17. H. V. SORENSEN, D. L. JONES, M. T. HEIDEMAN, AND C. S. BURRUS: *Real-valued fast Fourier transform algorithms.* IEEE Trans. Acoust., Speech, Signal Processing, vol. ASSP-35, pp. 849-863, June 1987.

18. G. M. HOOVER, J. G. GALLAGNER, H. K. RIGDON: *Vibrator signals.* Proceedings, vol. 72, pp. 1290-1315, October 1984.

19. P. S. SCHULTZ: *Seismic Velocity Estimation.* Proc. IEEE, vol. 72, no. 10, October 1984.

20. L. R. DENHAM: *Seismic interpretation.* Proc. IEEE, vol. 72, no. 10, October 1984.